J. Phys. B: At. Mol. Opt. Phys. **29** (1996) 4267–4283. Printed in the UK

Time-delay matrix analysis of resonances in electron scattering: e^-–H_2 and H_2^+

Darian T Stibbe† and Jonathan Tennyson†

Institute for Theoretical Atomic and Molecular Physics, Harvard-Smithsonian Center for Astrophysics, 60 Garden Street, Cambridge, MA 02138, USA

Received 13 June 1996

Abstract. In electron scattering from complex targets such as complex atoms or molecules, resonance features often occur at energies where the target has many excited electronic states. Standard methods of determining resonance positions and widths are unreliably close to electronic thresholds or fail when a resonance is too wide or found to overlap another resonance. By finding the time-delay matrix given by $\mathbf{Q} = -i\hbar\mathbf{S}^* \, \mathrm{d}\mathbf{S}/\mathrm{d}E$ it is possible to fit the resonance positions and widths more precisely and with greater certainty. It is also possible to find the 'branching ratios', the probabilities of decay of the resonance to the continuum of each target state. This helps in the accurate assignment of the resonance (particularly for core-excited shape resonances), reducing the extensive detective work that is often required. The usefulness of the time-delay matrix is demonstrated with two R-matrix electron–molecule scattering calculations: e^-–H_2 and e^-–H_2^+, although the method is not restricted to any particular type of calculation or target species. Resonance positions and widths are found for e^-–H_2^+. For the case of e^-–H_2, H_2^- resonances with $^2\Sigma_g$ symmetry are tracked as a function of bondlength. Their changing character is discussed and an avoided crossing at short internuclear separation is reported for the first time. The parentage of the 12 eV resonance has been classified as a $^3\Sigma_g$ contrary to previous classifications. Evidence of the notoriously shy series b resonances has been found.

1. Introduction

When an electron strikes an atom or molecule, it can, under certain conditions, be captured for a short time close to the target leading to the formation of a temporary compound state or resonance. Resonances associated with the target ground state occur because the incident electron is held within a penetrable potential barrier formed by the combination of centrifugal, polarization and exchange forces. These are known as shape resonances. Resonances associated with excited states consist of a hole in a normally occupied orbital and two electrons in normally unoccupied orbitals. These are known as core-excited resonances and fall into two categories. Feshbach resonances (Feshbach 1958, 1962) lie below their parent excited state and exhibit a positive electron affinity. Core-excited shape resonances, which are similar to the ground-state associated shape resonances, lie above their parent.

In the case of scattering by positively charged molecular ions, there will be a positive electron affinity and so Feshbach-type resonances are to be expected, with the resonances below the parent. For neutral molecules, Weiss and Krauss (1970) showed that Rydberg-excited states are also likely to have positive electron affinity and again, Feshbach resonances

† Permanent address: Department of Physics and Astronomy, University College London, London WC1E 6BT, UK.

0953-4075/96/184267+17$19.50

would be expected. Valence-excited states may have either positive or negative electron affinity and can result in either type of core-excited resonance. As will be demonstrated, for a molecule it is even possible for a resonance to move between the two types as the internuclear separation changes.

Feshbach resonances are forbidden from decaying into their parent by energy restrictions and must decay into lower target states. A shape resonance can feasibly decay into all lower target states but is most likely to decay into its parent. Studying the branching ratios of decay into the various continua gives useful information about the character of the resonance, as well as important physical information for modelling excitation processes.

The most common method of finding resonances is to look at the K-matrix or eigenphase sum. Standard programs such as RESFIT (Bartschat and Burke 1986), and RESON (Tennyson and Noble 1984) have been written for this purpose. A resonance will produce a characteristic form (Breit and Wigner 1936) in the eigenphase sum as a function of energy that can be fitted to find the position and width of the resonance. There are three complications that can thwart this. Firstly, it is often the case that the background varies so quickly and unpredictably that fitting can prove extremely difficult, particularly in the case of wide, short-lived resonances. Secondly, there can be two or more resonances in close proximity which, given the problems with the background, can result in poor fitting. Thirdly, resonances can be cut off by thresholds which can have the effect of distorting the resonance or of cutting off most of the characteristic form of the resonance. These effects make resonance fitting difficult. Many stable molecules have a forest of excited states in the 10 eV region; this region is well known experimentally to yield complicated, and often poorly understood, resonance structures (Schulz 1973) due to the proliferation of thresholds and multiple resonances.

Recently there have been several attempts to improve on traditional methods of resonance fitting. Quigley and Berrington (1996) used the properties of the R-matrix method in a procedure to fit automatically single or multiple resonances using the 'QB' method. Busby *et al* (1996) have written a graphical user interface to interactively zoom in on possible resonances which are then fitted using traditional methods. Spence and Scott (1996) borrowed the 'Hough transformation' from image processing to help detect resonances. Noble *et al* (1993) found resonance parameters by direct search of the complex $\boldsymbol{S}$ plane.

The time-delay method, using the time-delay matrix originated by Smith (1960) and used by Sadeghpour *et al* (1992) to study photodetachment of H^-, is based on the time delay experienced by the electron as it interacts with the target. At resonance, the time delay as a function of energy conforms to a characteristic shape which can be fitted to give the relevant parameters. This method affords considerable advantage and can remove or at least alleviate the problems associated with studying complicated resonance structures near thresholds. It is this method that we explore in this paper.

Section 2 gives the theory behind both the eigenphase sum and the time-delay methods for fitting resonances. In section 3, sample calculations of electron scattering from a molecular ion (H_2^+) are presented. Fits are performed using both methods and the results compared. The branching ratios are found and discussed. In section 4, calculations of scattering from the neutral H_2 molecule over a range of internuclear separations are presented. At the equilibrium separation, the resonances are fitted using both methods and the advantages of the time-delay method are discussed. The variation of the resonances as a function of bondlength is discussed in detail and the three resonances tracked are assigned to parent states. The branching ratios are also found and their significance and use outlined.

2. Theory of resonance fitting

2.1. Eigenphase sum method

Hazi (1979) showed that near an isolated multichannel resonance, the eigenphase sum as a function of energy, $\Delta(E)$, satisfies the formula due to Breit and Wigner (1936):

$$\Delta(E) = \Delta_0(E) + \tan^{-1}\left(\frac{\Gamma}{2(E_0 - E)}\right) \tag{1}$$

where Γ is the (total) width of the resonance and E_0 is its position. $\Delta_0(E)$ is the sum of the background phases which is usually assumed to be a low-order polynomial.

The value of the arctan function will change approximately from zero to π as E increases through E_0. For example, as E moves from, say, $(E_0 - 2\Gamma)$ to $(E_0 + 2\Gamma)$, the value of the function will increase by $\sim \frac{11}{13}\pi$. The position of the resonance lies at the point of inflection of the curve.

By fitting the eigenphase sum to this functional form, it should be possible to extract the resonance parameters. RESON (Tennyson and Noble 1984) is used here for this purpose. However, a problem can arise with the sum of the background phases, Δ_0. If the resonance is narrow, these will change little and can be set as a constant or modelled linearly. If on the other hand the resonance is wide, or if fitting is to be performed near a threshold, then the background can vary by a large and unpredictable amount. In this situation, use of high-order polynomials often leads to unreliable solutions. Typically the position of the resonance remains reasonably stable since the background would have to vary quite wildly to affect the point of inflection greatly, but the width of the resonance is more sensitive.

If two or more resonances overlap, the number of independent variables increases further and the results become very unreliable. Eigenphase fitting programs, such as RESON, work well for single, narrow resonances away from threshold. They tend to come unstuck, however, when trying to fit a double resonance. Under these circumstances, even the resonance positions are likely to be inaccurate.

2.2. Time-delay method

The delay time of a collision can be thought of classically as the difference between the total time the electron spends within a distance R of a target in the limit of $R \to \infty$ and the time it would have taken without any interaction. The quantum mechanical equivalent for steady-state wavefunctions is to take the particle density in the region around the target divided by the total flux, both with and without an interaction.

A method of finding these times was formulated by Smith (1960). The time-delay matrix $\mathbf{Q}$ is formed from the scattering matrix $\mathbf{S}$ and the time operator $-\mathrm{i}\mathrm{d}/\mathrm{d}E$ and is defined as

$$\mathbf{Q} = -\mathrm{i}\hbar\mathbf{S}^*\frac{\mathrm{d}\mathbf{S}}{\mathrm{d}E} \tag{2}$$

The largest eigenvalue of the $\mathbf{Q}$-matrix, q_{max}, represents the time delay experienced by the channel with the largest time delay and hence is sensitive to any resonances. Smith also showed that the probability of decay into a particular continuum, the branching ratio β, is given by the square of the corresponding component of the eigenvector associated with q_{max}.

At resonance, the maximum eigenvalue q_{max} has a Lorentzian form given by:

$$q_{max}(E) = \frac{\Gamma}{((E - E_0)^2 + (\Gamma/2)^2)}. \tag{3}$$

In the method developed here, the **Q**-matrix is found numerically by calculating the **S**-matrix just above and just below the energy E. We found this procedure was stable for energy differences in the range 0.1Γ to 0.01Γ. This is performed over a range of energies from which q_{max} is found as a function of energy. A plot of q_{max} is then examined for peaks that characterize a resonance. These are then fitted to find the resonance parameters. The method of fitting varies depending on whether the resonances are isolated or overlapping. If the resonances are isolated then each resonance is fitted independently to a Lorentzian form using a least-squares fitting routine. In these cases a small constant background is used to account for other far-away resonances. If there are two resonances overlapping, there are two methods for fitting them depending on their relative heights. If one is much narrower, then the narrower one is fitted first with a constant background and the wide one is then fitted to the eigenphase sum minus the fitted resonance. If the resonances are of similar height then they are fitted together as a double Lorentzian.

An important advantage of the Q-matrix method over eigenphase sum fits is that in the Q-matrix method only the channel with the longest time delay is fitted. This means that strongly varying but non-resonant channels do not need to be considered. This is particularly important for molecular targets as these have many degenerate channels.

Branching ratios can be found as a function of the electron energy. Useful information on the character of the resonance can be gained from the branching fraction as the electron energy passes through the resonant energy. For molecular calculations, the branching fractions at resonance as a function of internuclear separation can give insight into how the character of the resonance changes with bondlength.

3. Electron–H_2^+ scattering

R-matrix calculations were performed for the $^1\Sigma_g$ total symmetry at a bondlength of $R = 1.4\ a_0$, the equilibrium separation of H_2. The calculations used the wavefunctions developed and tested by Branchett and Tennyson (1992) and explicitly included three H_2^+ target states, $X\,^2\Sigma_g^+$, $A\,^2\Sigma_u^+$ and $B\,^2\Pi_u$ in the close-coupled expansions. The continuum electron was treated using a partial wave expansion which included partial waves with $l \leqslant 6$ in the external region. Further details of the calculation can be found in Tennyson (1996a).

The calculations reported here were performed as part of a wider study of superexcited states of H_2 as a function of internuclear separation, results of which are reported elsewhere (Tennyson 1996a). An important issue in these calculations is the branching ratio for the so-called Q_2 resonance series which converges to the $^2\Pi_u$ state of H_2^+ and, usually, can autoionize to either the ground $^2\Sigma_g^+$ state or the excited $^2\Sigma_u^+$ state of H_2^+.

Figure 1 shows the eigenphase sum and the time delay as a function of energy. In the eigenphase picture, the resolved resonances appear as a series of steps of π as the energy moves through each resonance in turn. As the resonances approach a threshold, their widths become so narrow that they begin to appear as characteristically shaped discontinuities. This effect is due to the energy resolution at which the calculation is executed and how the plotting of the eigenphase sum is performed. At the resonance position arbitary jumps by π in the eigenphase sum cause a discontinuity.

The resolved resonances in figure 1(a) are all dominantly p-wave in character; there are also f-wave and h-wave resonances but these are too narrow to be picked up at the resolution at which this calculation is performed. They can be seen more easily using the time-delay method.

In the time-delay picture, each resonance shows up as a Lorentzian with essentially no background and two distinct sets of Feshbach resonances can be seen. The Q_1 series

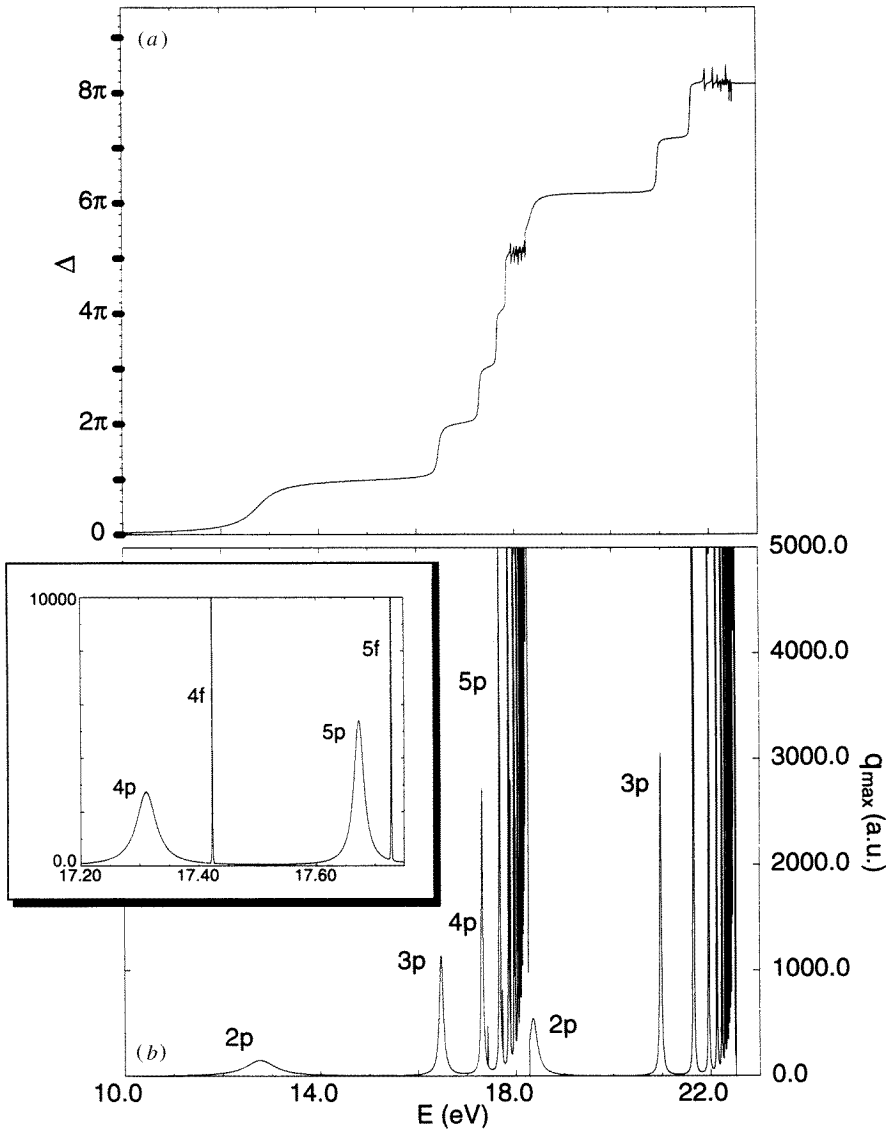

Figure 1. Electron–H_2^+ scattering at $R = 1.4\ a_0$, $^1\Sigma_g$ total symmetry: (*a*) Eigenphase sum (Δ) as a function of energy (E); (*b*) time-delay (q_{max}) as a function of energy (E). The inset, at higher resolution, shows the 4f and 5f resonances more clearly.

converges to the $^2\Sigma_u^+$ first excited state of H_2^+ and the Q_2 converges to the $^2\Pi_u$ state. Note that in the present calculations, the resonances can have up to three peaks, which can be assigned to their dominant partial waves, p, f and h, for each principal quantum number. The resonances associated with the f- and h-waves are sharp. The inset, which enlarges the 4p and 5p resonance regions, clearly shows the full Lorentzians of the 4f and 5f resonances.

Table 1 gives the resonance parameters found by using both methods for the first four resonances in the Q_1 series and the first resonance of the Q_2 series. The eigenphase sum is fitted using the program RESON (Tennyson and Noble 1984) and a linear background. The

Table 1. e^-–H_2^+ scattering at $R = 1.4\ a_0$, $^1\Sigma_g$ total symmetry: resonance positions and widths.

	Eigenphase method		Time-delay method	
	E_0 (eV)	Γ (eV)	E_0 (eV)	Γ (eV)
Q_1 series				
2p	12.7575	0.730 0	12.7572	0.730 17
3p	16.4750	0.095 20	16.4750	0.095 19
4p	17.3110	0.039 92	17.3110	0.039 91
4f	—	—	17.4230	0.000 04
5p	17.6730	0.020 20	17.6723	0.020 18
5f	—	—	17.7279	0.000 07
Q_2 series				
2p	18.3791	0.174 4	18.3604	0.199 5

f-wave resonances were not fitted by the eigenphase sum method. This method requires a closely spaced grid of eigenphases and thus becomes sensitive to any numerical noise in the eigenphases when the resonances are very narrow.

For the first series, the p-wave resonances are sharp enough such that even though they do begin to overlap as the thresholds are approached, both methods can fit them to a high degree of accuracy and give the same result to within 0.1%.

At $R = 1.4\ a_0$, the lowest resonance of the Q_2 series is cut off by the $^2\Sigma_g^+$ threshold at 18.27 eV. In this case, the shape of the resonance is not distorted by the cut-off when the time delay is viewed as a function of energy. This suggests there is very little interaction between the resonance and the $^2\Sigma_g^+$ target state. Nevertheless, the two methods give different results: (E_0, Γ) equals (18.379 eV, 0.1744 eV) for the eigenphase sum method and (18.360 eV, 0.1995 eV) for the time-delay method. Examining the fits in detail shows that the eigenphase sum method is having to contend with a large background, which is common close to threshold, so that its fit is subject to error. In contrast, the fit to the Lorentzian using the time-delay method is almost perfect and the result found is thus extremely reliable.

Figure 2 shows the branching fraction for decay into the ground state for the Q_2 series; the Q_1 series is below threshold and so all decay is into the ground state. It can be seen that when the energy passes through a p-wave resonance such as the one at energy 20.98 eV, there is almost no change in the branching fraction which stays at around 92%. On passing through an f-wave or h-wave resonance there is a sharp drop for the duration of the resonance. For the 4f resonance, the branching fraction is 77% and for higher nf resonances it goes down almost to zero (the calculation is not at high enough resolution to find exact values) which means it decays almost purely into the first excited $^2\Sigma_g^+$ state. The inset is a blowup of one of the spikes and shows that the $n = 5$ region does indeed contain two sharp resonances, one for the f-wave and one for the h-wave.

Analysis of a number of resonances and geometries shows that in general the branching ratio given by the dominantly p-wave resonances is close to the background value, but that the f- and h-wave resonances give branching ratios which differ significantly from this.

4. $^2\Sigma_g$ symmetry of electron–H_2 scattering

The calculations extend work performed by Branchett *et al* (1990) at a single internuclear distance and use the UK molecular *R*-matrix method (Gillan *et al* 1995). The target is

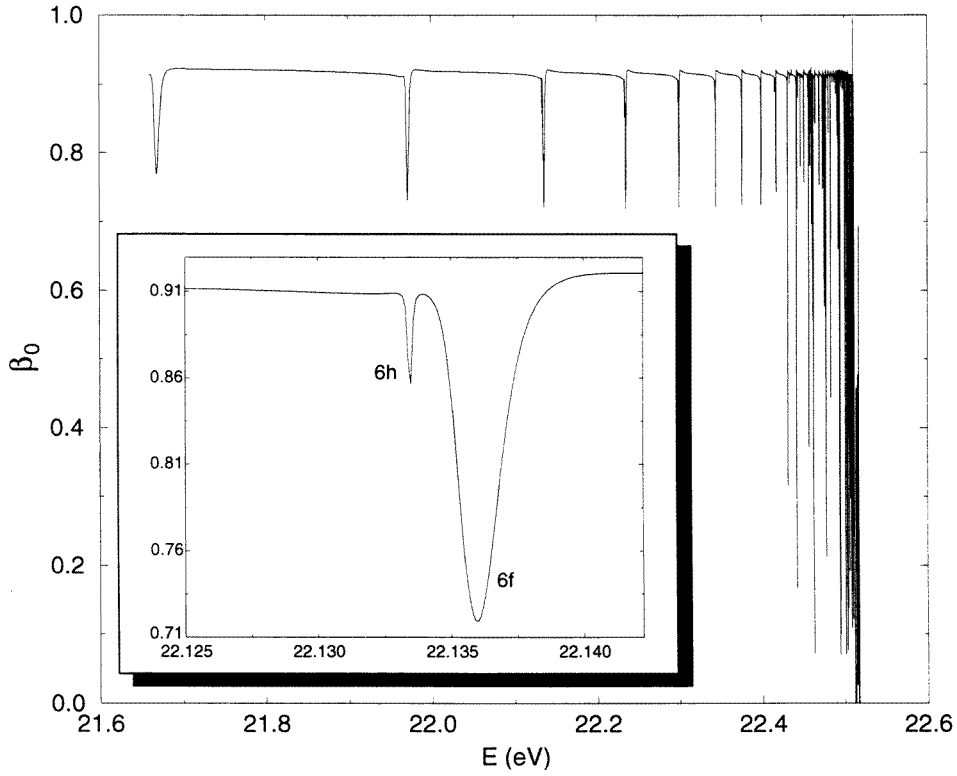

Figure 2. Electron–H_2^+ scattering at $R = 1.4\ a_0$, $^1\Sigma_g$ total symmetry. Branching fraction (β) of decay into the ground state as a function of energy. The inset, at higher resolution, shows the effect of the f- and h-wave resonances more clearly.

represented by the seven lowest states ($X\,^1\Sigma_g^+$, $b\,^3\Sigma_u^+$, $a\,^3\Sigma_g^+$, $c\,^3\Pi_u$, $B\,^1\Sigma_u^+$, $E, F\,^1\Sigma_g^+$ and $C\,^1\Pi_u$) and a full CI approach is used throughout. The model of Branchett *et al* (1990) has been improved significantly in the following ways.

(i) The target state basis functions have been re-optimized to give the best representation of the target over a range of internuclear separations.

(ii) The number of continuum basis functions per partial wave has been increased.

(iii) Phase inconsistencies between the original target CI vectors and the scattering target CI vectors have been removed using the method of Tennyson (1996b).

Other attempts to improve the quality of the model such as increasing the number of target basis functions and the number of target states considered are outside the remit of this paper and will be discussed elsewhere.

Procedures and results are discussed in detail at a single geometry, the H_2 equilibrium separation of $R = 1.4\ a_0$. Results of resonance fits using the time-delay method as a function of internuclear separation are then presented.

4.1. Equilibrium separation

Figure 3 shows the eigenphase sum and the time delay q_{max} with fitted Lorentzians at the equilibrium separation of $R = 1.4\ a_0$. From the eigenphase sums there appear to be two resonances between the first ($b\,^3\Sigma_u$) and the second ($a\,^3\Sigma_g$) thresholds. The first resonance

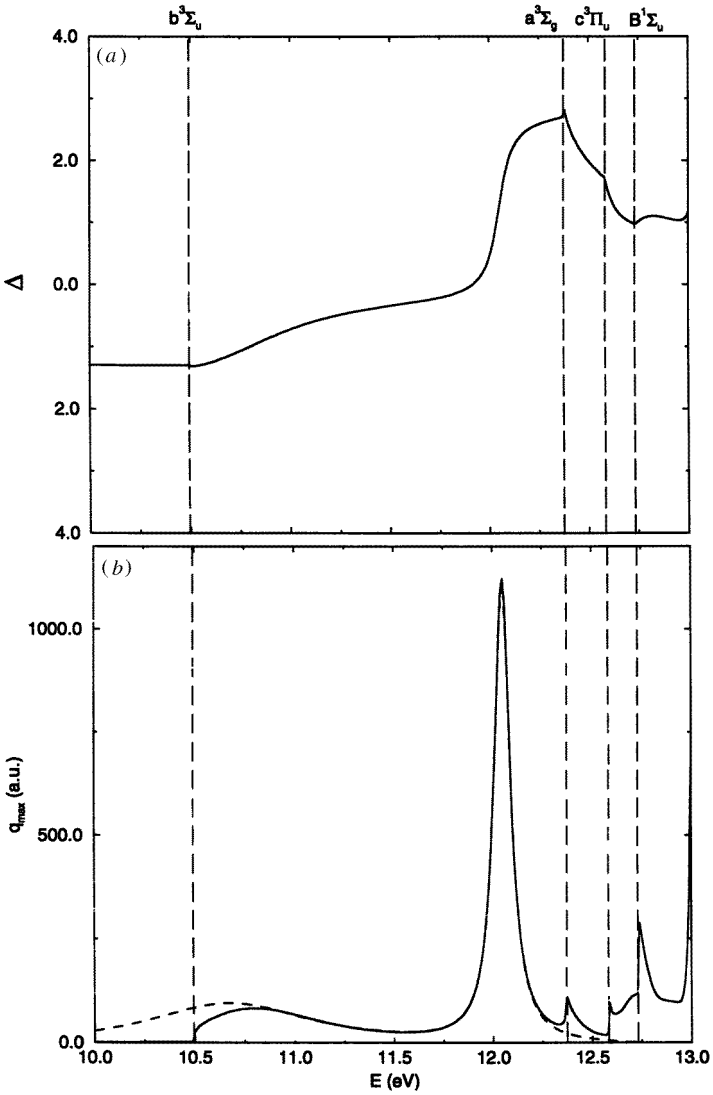

Figure 3. Electron–H_2 scattering at $R = 1.4\ a_0$, $^2\Sigma_g$ total symmetry. (*a*) Eigenphase sum (Δ) as a function of energy (E); (*b*) time delay (q_{max}) as a function of energy (E) with Lorentzian fit (broken line).

(res1) lies just above the $b\,^3\Sigma_u$ threshold and the eigenphase sum rises by less than $\pi/2$ rather than the expected π. This is partly because it is cut off by the threshold and partly because the background of the eigenphase sum tends to change rapidly at the thresholds. The second narrower resonance (res2), although also cut off by a threshold to higher energy, is accompanied by a rise of almost π in its eigenphase and is hence a much more pure resonance which should be easier to fit. Above the threshold at 12.3 eV there is a fair amount of structure but nothing that can clearly be called a resonance.

The existence of two, and only two, $^2\Sigma_g$ resonances below 12.3 eV is confirmed by the two clear peaks in figure 3(*b*), the time delay experienced by the electron. Res1 is a broad

Table 2. e^-–H_2 scattering at $R = 1.4\ a_0$, $^2\Sigma_g$ total symmetry: resonance positions and widths.

	Eigenphase method		Time-delay method	
	E_0 (eV)	Γ (eV)	E_0 (eV)	Γ (eV)
res1	10.677	1.555	10.673	1.035
res2	12.048	0.0973	12.049	0.0971

and thus short-lived resonance. As predicted from the eigenphase sum, it is cut off at low energy by the threshold. It is also seen that the shape of the left limb is distorted from a pure Lorentzian suggesting a strong interaction between the resonance and the target state. Res2 on the other hand is a narrow, long-lived resonance that is far enough away from any threshold to be undistorted close to its maximum, although it is distorted close to the a $^3\Sigma_g$ threshold. In the region near its maximum it is a near-perfect Lorentzian that can be fitted very well. As was seen in the eigenphase picture, above the 12.3 eV threshold there is much structure some of which could be due to resonances but the bunching of thresholds makes it impossible to resolve. This region will not be considered further.

For both resonances the eigenphase sums were fitted using RESON and a linear background. The time delay was fitted using a double-Lorentzian, least-squares fitting routine. For res1, the latter fitting was set to ignore the region near threshold where the Lorentzian is distorted. The parameters fitted with the two procedures are given in table 2.

The positions found by both methods for res1, which is a distorted resonance, are close (within 0.04%) but the fitted widths differ significantly, by ∼50%. This exemplifies the point mentioned previously, that the width fitted by the eigenphase sum method is always more sensitive to distortion than the position. The fit by the time-delay method is a much better one (in terms of residues to the expected form) and the results are thus more reliable.

In the case of res2 which suffers little distortion, both methods give almost the same position and widths.

In order to help clarify the parentage of the resonance, calculations using only two states, the ground and the candidate parent state, were performed. A ground state and b $^3\Sigma_u$ calculation was used as a test and as expected, res1 appeared but res2 did not. No trace of res1 was found in any of the other two-state calculations performed.

Conversely, a resonance appeared in the two-state calculations involving all four possible res2 parent states—c $^3\Pi_u$, C $^1\Pi_u$, a $^3\Sigma_g$ and E, F $^1\Sigma_g$. Fitting these resonances from the two-state calculations showed that the resonance position in the calculation involving the a $^3\Sigma_g$ state was 0.03 eV lower in energy than that found for res2 in the full seven-state calculation. The other two-state calculations gave resonance energies significantly higher.

The branching ratios, figure 4, show that res1 has more than a 90% chance of decaying into the continuum of the first excited state (b $^3\Sigma_u$). Res2 has an 85% chance of decay into this state.

4.2. As a function of internuclear distance

Calculations were performed at bondlengths between $R = 0.8\ a_0$ and $R = 4.0\ a_0$ at separations of $0.1\ a_0$. Res1 and res2 could be tracked over nearly the entire range of bondlengths. At long bondlength ($R > 3.0\ a_0$) a third resonance, res3, appears although it can be fitted only for $R \geqslant 3.7\ a_0$. All the resonances were fitted using the time-delay method. The eigenphase sum method proved inadequate whenever the resonance width

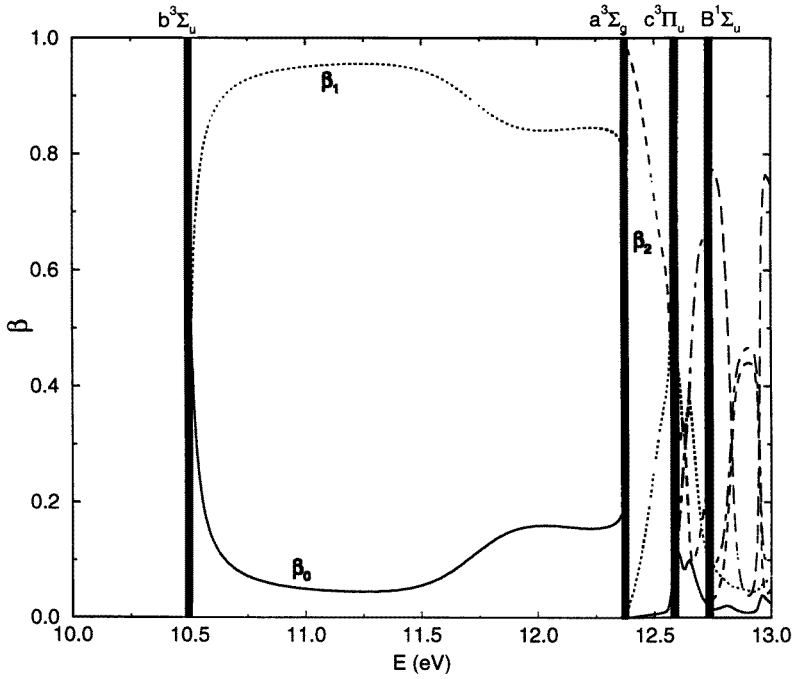

Figure 4. Electron–H_2 scattering at $R = 1.4a_0$, $^2\Sigma_g$ total symmetry. Branching ratios (β) as a function of energy (E). β_0 decays into the $X\,^1\Sigma_g$ state, β_1 into the $b\,^3\Sigma_u$ and β_2 into the $c\,^3\Sigma_g$.

became too large. Figure 5 shows how the positions of the resonances vary as a function of internuclear distance. They are plotted along with the excited target states with the energy relative to the ground state. Table 3 gives the positions, widths and branching ratios for res1 and res2 and table 4 gives the same information for res3.

From figure 5 it can be seen that res1 follows the $b\,^3\Sigma_u$ target state across the whole range of geometries. It lies above the threshold for nearly the entire range of bondlengths but moves below it for $R < 1.1\ a_0$. The most striking feature of figure 5 is the apparent avoided crossing between the resonances at $R \sim 1.2\ a_0$. It is this avoided crossing that is pushing the resonance below the $b\,^3\Sigma_u$ state at low internuclear separation.

Figure 6 shows how the width and branching ratios of res1 change as a function of geometry. For $R \leqslant 1.00$, the resonance is long lived and very narrow at around 0.02 eV. As it is below threshold, it can only decay to the ground state. As the separation increases, the resonance moves above threshold and the predominant decay is now to the $b\,^3\Sigma_u$ state (around 83%). The width also increases with separation up to a maximum of about 2.25 eV at $R \sim 2.0\ a_0$. In this region the resonance is very broad which makes it difficult and inaccurate to fit. The lack of smoothness in the curve in this region is a manifestation of this. On increasing the separation further, the width narrows and the branching fraction to the excited state drops until at $R = 4.0\ a_0$, the width is around 0.45 eV and the branching ratios are 56%:44% in favour of the first excited state.

It is impossible to track res2 across the whole range because it is cut off by the $a\,^3\Sigma_g$ threshold for $R < 1.1\ a_0$. At around $R = 3.6\ a_0$, it crosses the $E, F\ ^1\Sigma_g$ threshold which makes it difficult to fit due to other, non-resonant interactions with the threshold. It is not readily obvious which (if any) target-state curve the resonance is following.

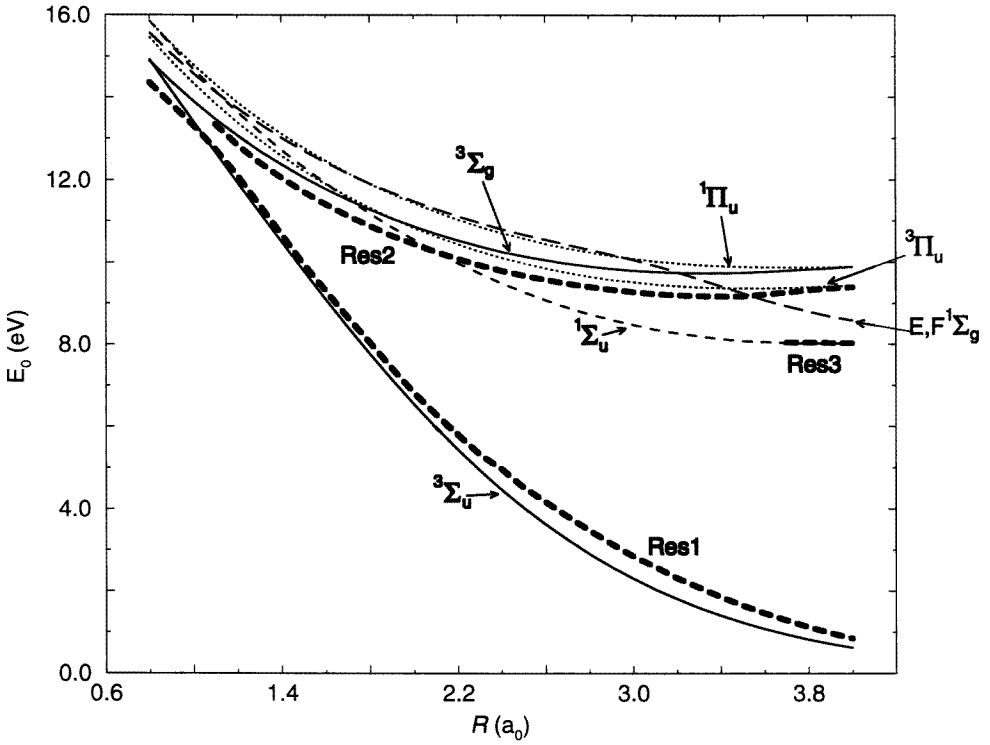

Figure 5. Electron–H_2 scattering for $^2\Sigma_g$ total symmetry: resonance positions E_0 and target state energies relative to the ground state as a function of bondlength (R).

Figure 7 shows the width and branching ratios of res2 as a function of bondlength. The resonance starts off at its broadest (around 0.42 eV) with the majority of decay into the b $^3\Sigma_u$ state (95%). As the bondlength increases, the width narrows and decay into the ground state X $^1\Sigma_g$ begins to predominate up to a maximum of 96% at around $R = 2.0\ a_0$. At $R = 2.1\ a_0$, res2 crosses the B $^1\Sigma_u$ threshold but is not greatly affected by it—its width does not change significantly and the branching ratios remain reasonably continuous. As R increases, the width begins to increase and the branching fraction to the B $^1\Sigma_u$ state increases at the expense of the other two ratios. After $R = 3.5\ a_0$, the resonance has crossed the E, F $^3\Sigma_g$ threshold which causes a jump in the width to around 0.30 eV before dropping again as the bondlength continues to increase. The branching fraction also shows a discontinuity due to the extra available decay state although decay into the B $^1\Sigma_u$ state still dominates (around 60%) with the newly available b $^3\Sigma_g$ taking around 30%.

A third resonance, res3, is only apparent at bondlengths $R \geqslant 3.0\ a_0$. For $R < 3.7\ a_0$ it is cut off by the B $^1\Sigma_u$ threshold at low energy before q_{max} reaches the maximum of the Lorentzian and table 4 shows the fitted parameters for $3.7\ a_0 \leqslant R \leqslant 4.0\ a_0$.

At $R = 4.0\ a_0$, the resonance is very sharp at $\Gamma = 0.016$ eV. As the bondlength decreases, the width rapidly increases and by $R = 3.7\ a_0$ it is already up to 0.24 eV. The branching ratios for $R = 3.7$, 3.8 and 3.9 a_0 give about an 85% decay into the $^1\Sigma_u$ state. For $R = 4.0\ a_0$, the fraction is only $\beta = 43\%$ but this is still the dominant decay.

Table 3. e^-–H_2 scattering, $^2\Sigma_g$ total symmetry: resonance positions, widths and branching fractions as a function of bondlength R for res1 and res2.

	Res1				Res2					
R (a_0)	E_0 (eV)	Γ (eV)	β_0	β_1	E_0 (eV)	Γ (eV)	β_0	β_1	β_2	β_3
0.80	14.371	0.0172	1.0	0.0						
0.90	13.835	0.0178	1.0	0.0						
1.00	13.316	0.0172	1.0	0.0						
1.10	12.745	0.0790	0.187	0.813	13.352	0.419	0.056	0.944		
1.20	12.110	0.361	0.071	0.929	12.848	0.289	0.073	0.927		
1.30	11.400	0.684	0.069	0.931	12.423	0.170	0.103	0.897		
1.40	10.673	1.035	0.092	0.908	12.049	0.0971	0.159	0.841		
1.50	9.952	1.279	0.128	0.872	11.712	0.0546	0.266	0.734		
1.60	9.297	1.591	0.138	0.862	11.407	0.0313	0.457	0.542		
1.70	8.650	1.831	0.152	0.848	11.129	0.0201	0.721	0.279		
1.80	8.044	2.098	0.153	0.847	10.878	0.0160	0.925	0.075		
1.90	7.417	2.192	0.169	0.831	10.640	0.0153	0.973	0.027		
2.00	6.815	2.138	0.183	0.827	10.440	0.0155	0.939	0.061		
2.10	6.292	2.228	0.171	0.829	10.252	0.0159	0.899	0.100	0.001	
2.20	5.793	2.051	0.162	0.838	10.083	0.0187	0.747	0.097	0.156	
2.30	5.317	1.920	0.155	0.845	9.931	0.0217	0.623	0.080	0.297	
2.40	4.969	2.036	0.129	0.871	9.796	0.0239	0.543	0.059	0.398	
2.50	4.523	1.838	0.128	0.872	9.677	0.0256	0.483	0.041	0.476	
2.60	4.164	1.800	0.120	0.880	9.572	0.0272	0.433	0.030	0.537	
2.70	3.819	1.689	0.116	0.884	9.480	0.0293	0.387	0.027	0.587	
2.80	3.479	1.565	0.117	0.883	9.402	0.0322	0.343	0.030	0.627	
2.90	3.156	1.422	0.121	0.879	9.335	0.0367	0.298	0.030	0.663	
3.00	2.857	1.301	0.128	0.872	9.281	0.0434	0.254	0.051	0.695	
3.10	2.596	1.222	0.138	0.862	9.237	0.0536	0.213	0.062	0.725	
3.20	2.322	1.070	0.153	0.847	9.205	0.0688	0.176	0.089	0.755	
3.30	2.092	0.990	0.171	0.829	9.184	0.0901	0.144	0.073	0.783	
3.40	1.862	0.888	0.195	0.805	9.174	0.1172	0.118	0.072	0.810	
3.50	1.653	0.802	0.222	0.778	9.172	0.1443	0.094	0.068	0.838	
3.60	1.463	0.728	0.253	0.747	9.221	0.3080	0.051	0.037	0.690	0.222
3.70	1.295	0.665	0.289	0.711	9.297	0.2677	0.047	0.030	0.633	0.290
3.80	1.126	0.583	0.331	0.669	9.331	0.2010	0.046	0.025	0.608	0.321
3.90	0.983	0.526	0.377	0.623	9.363	0.1698	0.046	0.024	0.592	0.338
4.00	0.849	0.466	0.428	0.572	9.394	0.1468	0.046	0.024	0.580	0.350

Table 4. e^-–H_2 scattering, $^2\Sigma_g$ total symmetry: resonance positions, widths and branching fractions as a function of bondlength for res3

R (a_0)	E_0 (eV)	Γ (eV)	β_0	β_1	β_2
3.70	8.0485	0.2391	0.056	0.073	0.871
3.80	8.0518	0.1333	0.053	0.066	0.881
3.90	8.0470	0.0611	0.084	0.101	0.815
4.00	8.0371	0.0156	0.265	0.303	0.432

4.3. The avoided crossing

To confirm that there is an avoided crossing between the two resonances, it is informative to look at the branching fractions as the bondlength decreases from around $R = 1.5\ a_0$. Res1 starts off dominated by decay into the $b\,^3\Sigma_u$ first excited state but as the bondlength

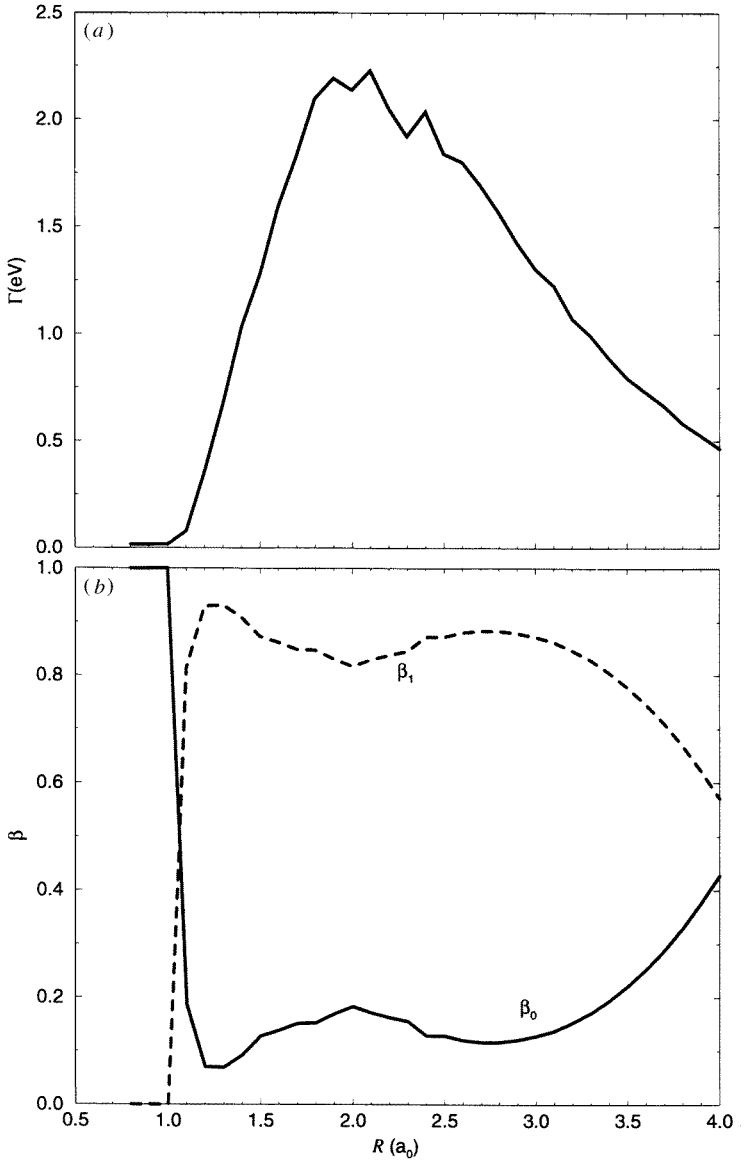

Figure 6. Electron–H_2 scattering, $^2\Sigma_g$ total symmetry. (*a*) Resonance width (Γ) and (*b*) branching fractions (β) for res1 as a function of bondlength (R). β_0 decays into the $X\,^1\Sigma_g$ state and β_1 into the $b\,^3\Sigma_u$.

decreases, the decay to the ground state becomes more likely. Unfortunately it is just at this point that the resonance crosses the $b\,^3\Sigma_u$ threshold so that the branching fraction to the ground state is forced to be unity which makes it harder to confirm this trend. In contrast, for res2, the branching ratio does the opposite, at high R dominated by decay into the ground state but on decreasing the bondlength, it becomes dominated by decay into the $b\,^3\Sigma_u$ state. This apparent swapping of characteristics between the two resonances is exactly what would be expected at an avoided crossing.

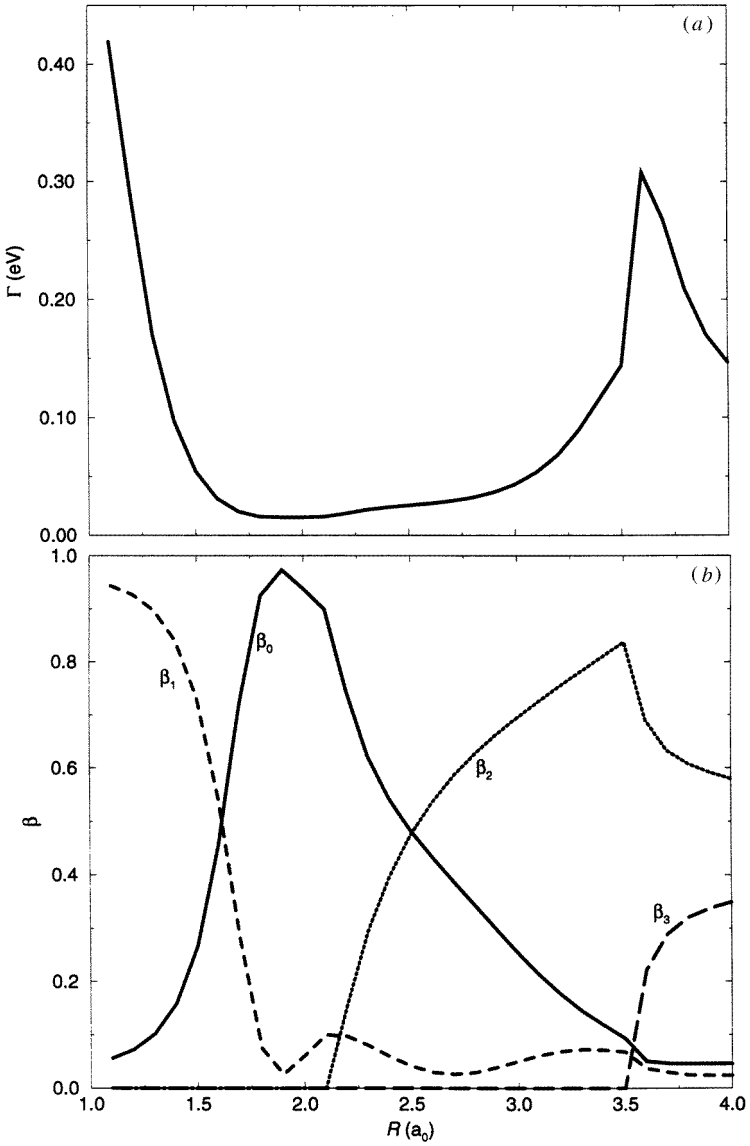

Figure 7. Electron–H_2 scattering, $^2\Sigma_g$ total symmetry. (*a*) Resonance width (Γ) and (*b*) branching fractions (β) for res2 as a function of bondlength (R). β_0 decays into the $X\,^1\Sigma_g$ state, β_1 into the $b\,^3\Sigma_u$, β_2 into the $B\,^1\Sigma_u$ and β_3 into the E, $F\,^1\Sigma_g$.

4.4. Assignment of the resonances

The assignment of resonances in the 10–13 eV region has been extensively discussed in a review paper by Shultz (1973).

There is general agreement that there exists a resonance at around 10 eV that can be identified as the $(1\sigma_g^1, 1\sigma_u^2)$ repulsive state of H_2^- (Comer and Read 1971, Eliezer *et al* 1967, Sharp 1971). This has the first excited state ($b\,^3\Sigma_u$) as its parent.

Our res1 clearly corresponds to the $(1\sigma_g^1, 1\sigma_u^2)$ state, in particular.

(i) In figure 3(*b*), the time delay at the equilibrium geometry, res1, was distorted by the $b\,^3\Sigma_u$ threshold suggesting a strong interaction which would be expected between a parent and daughter.

(ii) The branching ratios across almost the entire range of bondlengths show that the resonance is overwhelmingly likely to decay into the $b\,^3\Sigma_u$ state.

(iii) When res1 is plotted as a function of bondlength it closely follows the $b\,^3\Sigma_u$ state over the entire range.

The assignment of resonances in the region around res2 is less clear. In their experiment, Comer and Read (1971) saw three narrow resonances which formed vibrational series. They termed these series *a*, *b* and *c*, which is the notation that has been followed since (Schultz 1973, Mason and Newell 1986). Theory (Branchett and Tennyson 1990) suggests that series *c* is $^2\Pi_u$ symmetry and is not discussed here. Series *b* will be discussed in relation to res3.

Res2 in absolute energy as a function of bondlength closely follows the series *a* H_2^- potential curve found by Comer and Read (1971) and Joyez *et al* (1973). The minima of these potentials were found at $1.83 \pm 0.02\ a_0$ and $1.85 \pm 0.04\ a_0$, respectively, in very good agreement with the minimum of the absolute resonance energy found in this work of $1.87\ a_0$.

Eliezer *et al* (1967) gave the possible parent states of series *a* resonances as $c\,^3\Pi_u$, $C\,^1\Pi_u$, $a\,^3\Sigma_g$ and E, $F\,^1\Sigma_g$. This is confirmed by the two-state calculations performed here in which resonances appeared for all of these candidate parents. A resonance also appeared in a five target state calculation, using the Schwinger multichannel method by da Silva *et al* (1990). The calculation did not include the Π target states and represented the E, $F\,^1\Sigma_g$ state by only the $E\,^1\Sigma_g$ inner section and so this resonance's identification as a $^3\Sigma_g$ does not help in the positive identification of res2. Comer and Read (1971), by comparing their observed resonant state with potential curves found by Sharp (1969), concluded that only the $a\,^3\Sigma_g$ and the $c\,^3\Pi_u$ are possible. For the $C\,^1\Pi_u$, the energy difference between resonance and parent is too great and the shape of the resonance curve is not consistent with an E, $F\,^1\Sigma_g$ parentage. The same conclusion is reached in this work. In their calculation, Eliezer *et al* (1967) found that the lowest $^2\Sigma_g$ state of H_2^- was $c\,^3\Pi_u$ and so Comer and Read chose this state as the parent for the resonance. However, the calculations performed here suggest that the $a\,^3\Sigma_g$ is in fact the parent for the following reasons.

(i) Until distorted by the avoided crossing, the shape of res2 follows the $a\,^3\Sigma_g$ potential much more closely than the $c\,^3\Pi_u$ particularly at longer bondlength, and they have minimum points within $0.01\ a_0$ of each other.

(ii) At $R = 1.4\ a_0$, two-state calculations show that when the $a\,^3\Sigma_g$ state was included, a resonance appeared at energy 0.03 eV below the position of res2. The inclusion of all seven states gives rise to res1 which would push the resonance up slightly to the position of res2 due to the avoided crossing. The resonance found in the two-state calculation including the $c\,^3\Pi_u$ state gives an energy 0.15 eV above that of res2 which would be pushed even further away by the inclusion of res1.

Series *b* is somewhat harder to see both theoretically and experimentally. Comer and Read (1971) saw resonances appearing in high-vibrational exit channels but they did not see them in a later experiment (Joyez *et al* 1973) as they were outside the range of observation. Huetz and Mazeau (1981) did assign one of their observations to series *b* but Mason and Newell (1986) did not observe any series *b* resonances. On the theoretical side, Branchett and Tennyson (1990) and Branchett *et al* (1990) did not find any evidence of a series *b* resonance in their calculation performed at a single bondlength. Comer and Read (1971) assigned the resonances series *b* to a $^2\Sigma_g$ resonance with the parent state $B\,^1\Sigma_u$.

Res3 appears at long bondlengths in our calculations, tracking just above the $B\,^1\Sigma_u$ target state. This, along with the fact that decay of the resonance is dominated by decay

into this state is consistant with Comer and Read's resonance *b*. The resonance does not appear at shorter bondlengths in our calculations and those of Branchett and co-workers for the following reason. From the correlation diagrams of Sharp (1971), the resonance appears to be correlated asymptotically with the F $^1\Sigma_g$ state of H_2. In these calculations, the E, F $^1\Sigma_g$ target state, but no higher $^1\Sigma_g$ states, is included in the close-coupling model. It seems that at long bondlength, when the first excited $^1\Sigma_g$ state has almost pure F-state character, the resonance appears. At lower bondlength where the character is more of the E state, the resonance no longer appears.

If this supposition is correct then the inclusion of further $^1\Sigma_g$ excited states in the calculation ought to stabilize this resonance at shorter bondlengths. Unfortunately the next excited $^1\Sigma_g$ state lies in a region with many, spatially extended, excited states. It seems unlikely that the present techniques can cope with such target state expansions. Similar problems have been encountered in calculations studying electron collisions with CO (Morgan and Tennyson 1993).

5. Conclusions

The time-delay method can be used in any calculations in which it is possible to find the *S*-matrix as a function of energy. It provides a way of fitting resonances in difficult situations where the standard eigenphase sum fitting methods fail. These situations tend to occur at energies near to thresholds, when multiple resonances overlap, or when the resonance is very wide.

In the case of e–H_2^+ scattering, the time-delay method and the eigenphase sum method gave the same results for the first Rydberg series, in which the resonances are all quite narrow and away from threshold. The time-delay method proved essential, however, in fitting the first resonance (2p) of the second Rydberg series. The eigenphase method was thrown both by the large, varying background near the threshold and the fact that the resonance is cut off by the threshold. Neither of these problems affected the time-delay method.

For e–H_2 scattering, the eigenphase method was found to be inadequate due to the complexity of the resonance structure. In particular, when the resonances became very wide, even if the method managed to find the resonance position, the widths were found to be extrememly inaccurate. The time-delay method fitted even the widest (2.4 eV) resonances although at this width (and due to threshold distortions) the accuracy is reduced.

In many cases, when the resonance was near the threshold, it was impossible to fit it using the eigenphase method. Without the time-delay method, the resonances could not have been tracked across the whole range of bondlengths.

The branching ratios that come out of using the time delay, and other (Barschat and Burke 1986, Quigley and Berrington 1996) methods can prove extremely useful. In particular, finding the greatest branching ratios should identify immediately core-excited (i.e. above threshold) resonances. They cannot be used to identify Feshbach (below threshold) resonances without other evidence as they cannot decay into their parent.

An avoided crossing between resonances in e^-–H_2 scattering was found at low internuclear distances. The parent state of the resonance in the 12 eV region was classified as a $^3\Sigma_g$, contrary to previous classifications, although the resonance also showed significant interactions with three other states which have been discussed before as possible parents. For the first time in this type of calculation, evidence for the series *b* resonance as seen experimentally by Comer and Read (1971) has been found.

A full study of resonances as a function of internuclear separation in e^-–H_2 for all low-lying symmetries is currently being performed; results will be reported in this journal.

Acknowledgments

We would like to thank Hossein Sadeghpour for many helpful discussions and everyone at ITAMP for their hospitality during the course of this work. This work was supported by the US National Science Foundation through a grant for ITAMP at Harvard University and Smithsonian Astrophysical Observatory, and the UK Engineering and Physical Science Research Council.

References

Bartschat K and Burke P G 1986 *Comput. Phys. Commun.* **41** 75
Branchett S E and Tennyson J 1990 *Phys. Rev. Lett.* **64** 2889
——1992 *J. Phys. B: At. Mol. Opt. Phys.* **25** 2017
Branchett S E, Tennyson J and Morgan L A 1990 *J. Phys. B: At. Mol. Opt. Phys.* **23** 4625
Breit G and Wigner E P 1936 *Phys. Rev.* **49** 519, 642
Busby D W, Scott N S, Burke P G, Burke V M and Noble C J 1996 *23rd ATMOP Conf. (Oxford, 1996)* Abstracts (see also http://www.cs.qub.ac.uk/∼D.Busby/analysis.html)
Comer J and Read F H 1971 *J. Phys. B: At. Mol. Phys.* **4** 368
da Silva A J R, Lima M A P, Brescansin L M and McKoy V 1990 *Phys. Rev.* A **41** 2903
Eliezer I, Taylor H S and Williams J K 1967 *J. Chem. Phys.* **47** 2165
Feshbach H 1958 *Ann. Phys., NY* **5** 357
——1962 *Ann. Phys., NY* **19** 287
Gillan C J, Tennyson J and Burke P G 1995 *Computational Methods for Electron Molecule Collisions* ed W M Huo and F Gianturco (New York: Plenum) pp 239–52
Hazi A J 1979 *Phys. Rev.* A **19** 920–2
Joyez G, Comer J and Read F H 1973 *J. Phys. B: At. Mol. Phys.* **6** 2427
Mason N J and Newell W R 1986 *J. Phys. B: At. Mol. Phys.* **19** L587
Morgan L A and Tennyson J 1993 *J. Phys. B: At. Mol. Opt. Phys.* **26** 2429
Noble C J, Dörr M and Burke P G 1993 *J. Phys. B: At. Mol. Opt. Phys.* **26** 2983
Quigley L and Berrington K A 1996 *J. Phys. B: At. Mol. Opt. Phys.* submitted
Sadeghpour H R, Greene C H and Cavagnero M 1992 *Phys. Rev.* A **45** 1587
Schulz G J 1973 *Rev. Mod. Phys.* **45** 423
Sharp T E 1969 Publication LMSC 5-10-69-9, Lockheed Research Lab., Palo Alto, California
——1971 *At. Data* **2** 119
Smith F T 1960 *Phys. Rev.* **114** 349
Spence I T and Scott N S 1996 *PECAM II, (Belfast, 1996)* Abstracts
Tennyson J 1996a *At. Data Nucl. Data Tables* in press
——1996b *Comput. Phys. Commun.* submitted
Tennyson J and Noble C J 1984 *Comput. Phys. Commun.* **32** 421
Weiss A W and Krauss M 1970 *J. Chem. Phys.* **52** 4363